Science of the Total Environment 876 (2023) 162771

Contents lists available at ScienceDirect

Science of the Total Environment

journal homepage: www.elsevier.com/locate/scitotenv

Thresholds for triggering the propagation of meteorological drought to hydrological drought in water-limited regions of China

Qiang Liu [a,b], Yuting Yang [c], Liqiao Liang [d,*], He Jun [e], Denghua Yan [f], Xuan Wang [a,b], Chunhui Li [a,b], Tao Sun [a,b]

[a] State Key Laboratory of Water Environment Simulation, School of Environment, Beijing Normal University, Beijing 100875, China
[b] Key Laboratory for Water and Sediment Sciences, Ministry of Education, School of Environment, Beijing Normal University, Beijing 100875, China
[c] State Key Laboratory of Hydroscience and Engineering, Department of Hydraulic Engineering, Tsinghua University, Beijing, China
[d] State Key Laboratory of Tibetan Plateau Earth System, Environment and Resources (TPESER), Institute of Tibetan Plateau Research, Chinese Academy of Sciences, Beijing 100101, China
[e] General Institute of Water Conservancy and Hydropower Planning and Design, Ministry of Water Resources, Beijing, China
[f] State Key Laboratory of Simulation and Regulation of the Water Cycle in River Basins, China Institute of Water Resources and Hydropower Research, Beijing 100038, China

HIGHLIGHTS

- The propagation thresholds trigger drought transition.
- Drought events were assessed by pooling, excluding, and matching them by run theory.
- Propagation thresholds were defined by Copula function combined with transpose time.
- Hydrological drought tends to be amplified than its triggering ones.
- Shorter transpose time implies higher propagation thresholds.

GRAPHICAL ABSTRACT

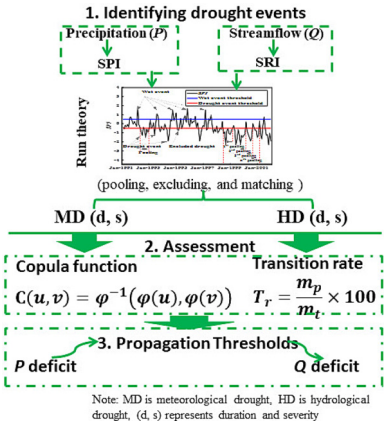

ARTICLE INFO

Editor: Ashantha Goonetilleke

Keywords:
Meteorological drought
Hydrological drought
Drought propagation
The Loess Plateau
Copula

ABSTRACT

Propagation thresholds that trigger a transition between meteorological drought and hydrological drought are poorly understood, which hinders effective establishment of drought warning systems and prevention measures. Here, propagation thresholds were assessed by firstly identifying drought events during 1961–2016 in the Yellow River Basin, China, subsequently pooling, excluding, and matching them, and finally assessing their threshold conditions by using a combined Copula function and transition rate (T_r) analysis. These results show that response time changed according to variations in drought duration and watershed characteristics. Importantly, response times increased according to the timescales over which they were studied; for example, the Wenjiachuan watershed recorded response times of 8, 10, 10, and 13 months when examined at 1-, 3-, 6-, and 12-month timescales, respectively. Additionally, the severity and duration of meteorological and hydrological drought events both increased when events were combined rather than studied individually. These effects were also amplified for matched meteorological and hydrological droughts by factors of 1.67 (severity) and 1.45 (duration), respectively. Shorter response times were identified in the Linjiacun (LJC) and Zhangjiashan (ZJS) watersheds, and correlated with their relatively small T_r values of 43 % and 47 %, respectively. Higher propagation thresholds for drought characteristics (*e.g.*, 1.81 and 1.95 for drought severity in the LJC and ZJS watersheds, respectively) imply that shorter response times tended to have greater effects on

* Corresponding author at: Institute of Tibetan Plateau Research, Chinese Academy of Sciences, Beijing 100101, China
E-mail addresses: qiang.liu@bnu.edu.cn (Q. Liu), liangliqiao@itpcas.ac.cn (L. Liang).

http://dx.doi.org/10.1016/j.scitotenv.2023.162771
Received 15 January 2023; Received in revised form 11 February 2023; Accepted 6 March 2023
Available online 11 March 2023

hydrological drought events and lowered their T_r, and *vice versa*. These results provide new insight into propagation thresholds used for water resource planning and management, and may help to mitigate the effects of future climate change.

1. Introduction

The intensity and frequency of droughts are both expected to increase as climate change becomes more severe (Dai, 2012; Trenberth et al., 2013; Yang et al., 2020; Yan et al., 2021; Satoh et al., 2022). No formal definition exists for a drought, although such events are usually defined as 'a prolonged period of abnormal precipitation shortage', and are characterized by a severe shortage of water in one section of the water cycle (Van Loon et al., 2016). Lack of a formal definition for drought stems from the diversity of drought indices, which generate significant uncertainty in quantitative assessments (Satoh et al., 2021). Generally, droughts are classified into four types: Meteorological drought, hydrological drought, agricultural drought, and socioeconomic drought (American Meteorological Society, 1997; Dai et al., 2020). Strong linkages that exist between different types of drought have generated much attention in the scientific community. In this context, different drought indices have been developed for representing drought, such as the standardized precipitation index (SPI) (McKee et al., 1993), Palmer Drought Severity Index (PDSI) (Palmer, 1965), the soil moisture drought index (Samaniego et al., 2013), and standardized runoff index (SRI) (Shukla and Wood, 2008). However, different drought indices, considered specific hydroclimatic processes and its low intersubstitutability between each other, have been selected to elucidate the drought characteristics using linear or nonlinear multivariate methods (Azhdari et al., 2020, 2021; Satoh et al., 2021). Furthermore, previous researchers have attempted to elucidate different type drought transitional characteristics, including defining drought propagation thresholds and major influencing factors (*e.g.*, Apurv et al., 2017; Wu et al., 2018; Apurv and Cai, 2020; Zhou et al., 2021; Yin et al., 2022a). Differences in climate and watershed characteristics inevitably induce greater uncertainty in understanding drought propagation, especially for the transition from meteorological to hydrological drought, which typically has the largest influence on effective management of water resources in a region.

The propagation from meteorological to hydrological drought involves changing a range of complex catchment and climate characteristics (*e.g.*, Tallaksen et al., 2009; Apurv et al., 2017; Konapala and Mishra, 2020). As pointed out by Peterson et al. (2021), watersheds can have a limited resilience to disturbances, which suggests that hydrological droughts can persist indefinitely after a meteorological drought ends (Peterson et al., 2021). This inevitably induces a shift in the relationship between precipitation (P) and streamflow (Q), and may also indicate that multiple steady states can exist in a watershed (Saft et al., 2016; Wu et al., 2021a). Key drought characteristics (*i.e.*, magnitude and duration) vary according to climate and catchment characteristics, such as attenuation, amplification, lag, and prolongation (*e.g.*, Yang et al., 2017; Guo et al., 2020; Peterson et al., 2021). Apurv et al. (2017) characterized drought propagation mechanisms into the following three types: (*i*) those involving seasonal groundwater recharge cycles that persist during periods of low rainfall, (*ii*) those characterized by seasonal groundwater recharge cycles that are suppressed during periods of low rainfall, and (*iii*) those exemplified by a lack of seasonality in groundwater recharge and where P has a strong control on groundwater recharge. Each of the above mechanisms causes hydrological drought to have a shorter, longer, and similar duration to meteorological drought, respectively. Furthermore, differences in climatic characteristics (*e.g.*, timing of P and climate aridity) combined with differences in vegetation responses triggered by a reduction in P in regions of different aridity serve to increase complexity in drought propagation modeling (Vicente-Serrano et al., 2012; Apurv et al., 2017). For example, vegetation in arid and humid zones responds to drought at relatively shorter timescales than vegetation in semi-arid and sub-humid zones, primarily due to their different regulating mechanisms (Vicente-Serrano et al., 2012). This implies that different hydrological effects are induced by different changes in vegetation, such as increasing evapotranspiration due to vegetation growth, which causes Q to decrease (Wang and Wang, 2018), or an increased infiltration induced by a greater rooting depth, which causes Q to increase (*e.g.*, Han et al., 2021). Furthermore, the terms 'response time', 'time lag', and 'propagation threshold' have been used to define processes associated with the propagation from meteorological to hydrological drought. These terms have historically been used interchangeably (Wu et al., 2021b) and have been traditionally defined by three methods (Wu et al., 2021b): The run theory method (*e.g.*, Yevjevich, 1967; Wu et al., 2021b), the correlation analysis method (Wu et al., 2018), and the non-linear response method (Wu et al., 2017). Here, response time was used to describe the magnitude and extent of meteorological drought; lag time is defined as the difference between the beginning and end of the period between meteorological and hydrological droughts; and propagation threshold is regarded as the intensity and duration of a meteorological drought that is needed to trigger a hydrological drought. A sequence of drought event is multivariate random process with multivariate dependence, indicating truncated event can affect each other (Chang et al., 2016; Tu et al., 2018). Copula functions, which can model random variables and their dependence, and multivariate joint distributions, as well as their joint return periods, have been widely used in multivariate drought studies (*e.g.*, Chang et al., 2016; Tu et al., 2018; Guo et al., 2020; Wu et al., 2022a). Meanwhile, variation in drought propagation characteristics (*e.g.*, amplification effects, lag time, and propagation threshold) reflect the complexity of natural systems, although the propagation thresholds for individual watershed characteristics, even in the same arid regions, remain uncertain (*e.g.*, Guo et al., 2020; Wu et al., 2021a, 2021b; Wu et al., 2022b; Satoh et al., 2022). Consequently, the objectives of this study were to: (*i*) quantify the individual response times of hydrological and meteorological drought events; (*ii*) assess the characteristics of propagation from meteorological drought to hydrological drought; and (*iii*) define the propagation threshold by considering the transition rate (T_r) in different watersheds of the Yellow River Basin, which is a typical water-limited basin in China. Due to complexity in drought propagation analysis, run theory has been employed to identify drought events, subsequently pooled, excluded, and matched them, and then performed a novel threshold assessment by combining the Copula function with T_r. Details are provided in the Method section.

2. Methods and materials

2.1. Study area

The Yellow River is approximately 5, 400 km long and drains an area of 795, 000 km^2. It originates on the Tibetan Plateau, flows through the Loess Plateau and North China Plain, and terminates in the Bohai Sea (Fig. 1). It exhibits a continental temperate climate and has two distinct seasons, with mean annual average, minimum, and maximum air temperatures of 7.9, 1.9, and 14.4 °C, respectively (Liang et al., 2014; Liu et al., 2016). Drought events caused by climate change and anthropogenic activities have had significant impacts on the Yellow River. For example, decreasing trends in P have been observed at most stations within the Yellow River Basin (YRB) over the previous 50 years (Liu et al., 2008; Liang et al., 2015). Furthermore, revegetation activities, such as the "Grain for Green" program conducted on the Loess Plateau (McVicar et al., 2007; McVicar et al., 2010), have dramatically increased the vegetation cover from 8.19 % to 15.82 % (Piao et al., 2015), which is approaching the limit for keeping water resources sustainable (Feng et al., 2016). As such, the YRB has been affected

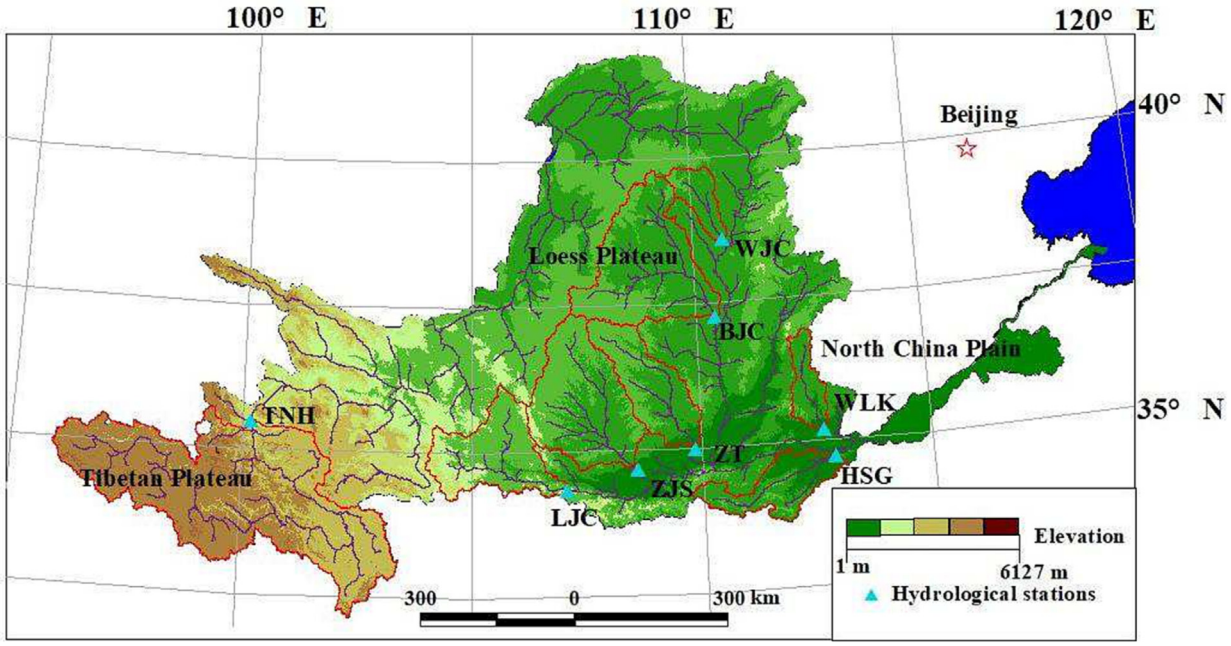

Fig. 1. Locations of the studied catchment areas of the Yellow River, China. Watershed abbreviations are as follows: Tangnaihang (TNH), Wenjiachuan (WJC), Baijiachuan (BJC), Linjiacun (LJC), Zhangjiashan (ZJS), Zhuangtou (ZT), Heishiguan (HSG), and Wulongkou (WLK).

by a series of drought events that have impacted local hydrological (*e.g.*, Wu et al., 2018; Guo et al., 2020) and socioeconomic systems (*e.g.*, Guo et al., 2019a, 2019b).

2.2. Method

(1) Drought indices

The standardized precipitation index (SPI) and standardized runoff index (SRI) have been widely used in drought frequency analysis and drought risk management, largely owing to their ease of calculation and ability to work over multiple timescales (Palmer, 1965; McKee et al., 1993; Hao et al., 2014; Farahmand and AghaKouchak, 2015; Guo et al., 2020). By considering the definition of drought, thresholds SPI and SRI were set during dry and wet events to −0.5 and 0.5, respectively (Madadgar et al., 2017; Guo et al., 2020). The response time of hydrological drought to meteorological drought was calculated using correlation analysis performed at 1-, 3-, 6-, and 12-month timescales (*e.g.*, Wu et al., 2018; Wu et al., 2021b). Given potentially large overlaps in drought events and deviations in duration that may result from modeling multiple timescales (Guo et al., 2020; Satoh et al., 2021), SPI and SRI values for a 1-month timescale analysis were used to quantify the response time, and then used to identify matching meteorological and hydrological droughts. The severity and duration of a drought event are some of the most important parameters that can be used to describe and classify it, and were therefore used in this study (Sadeghipour and Dracup, 1985; Huang et al., 2016). Meteorological and hydrological droughts were identified by using run theory (Yevjevich, 1967), and individual drought events were defined by their threshold, duration, and severity (Montaseri et al., 2018; Guo et al., 2020). The pooling and exclusion method for identifying drought events was initially proposed by Zelenhasić and Salvai (1987), but later was revised by Madsen and Rosbjerg (1995). It is widely used when defining drought events by considering multiple drought characteristics (Tu et al., 2018, 2019; Guo et al., 2020) and was adopted here for quantification purposes.

Firstly, the criteria used for drought pooling were constructed based on inter-event times and volumes. Specifically, conditions should be determined whether (*i*) two adjacent drought events $\{d_i, s_i\}$ and $\{d_{i+1}, s_{i+1}\}$ had an interval time t_i less than the predefined critical duration t_c, and if (*ii*) the ratio p_i of the inter-event excess volume above the threshold v_i to the preceding loss volume s_i was less than the predefined critical value p_c. If both criteria were true, both drought events were pooled into one new drought event:

$$\begin{cases} d_{pooled} = d_i + d_{i+1} + t_i \\ s_{pooled} = s_i + s_{i+1} + v_i \end{cases} \quad (1)$$

where d_{pooled} and s_{pooled} denote the drought duration and severity, respectively, after two adjacent drought events were pooled. As shown in Fig. 2, the pooling process was continued by using Eq. (1) until $t_i > t_c$ or $p_i > p_c$.

Secondly, several drought events that had short durations and minor severities, even after pooling, did not affect the underlying surface and hydrological conditions of the watershed, such that there was no disruption to drought properties in our statistical analysis model. As such, drought exclusion method of Tallaksen et al. (2009) was employed, whereby two critical

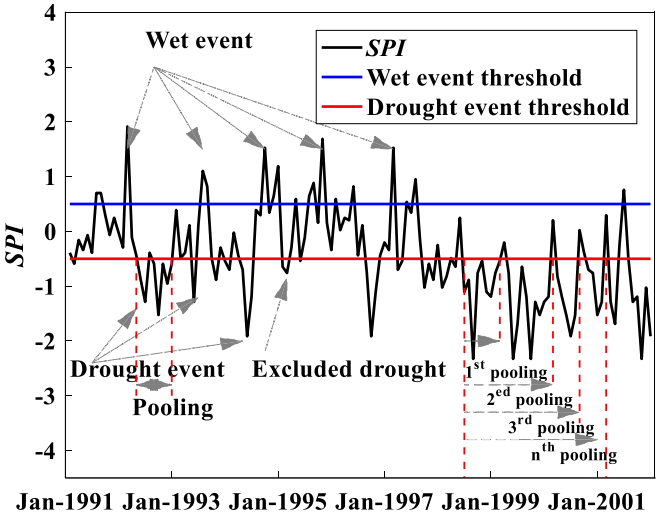

Fig. 2. The processes of identifying meteorological and hydrological drought events by run theory. Values for SPI from the WJC watershed from January 1991 to December 2001 are used for illustration.

ratios r_d and r_s were predefined to represent the percentiles of the mean value of droughts with durations d_{ave} and s_{ave}, respectively. If drought duration d_i was less than $r_d \times d_{av}$ or drought severity s_i was less than $r_s \times s_{ave}$, the drought events $\{d_i, s_i\}$ were excluded.

Duration and severity are two important characteristics of drought events, and can be used to uniquely describe any single drought event. Nonetheless, when classifying drought events, drought duration and severity are equally important (Guo et al., 2019a), such that modeled results are only reliable when r_d is equal to r_s. In other words, r_d and r_s are essentially the same for a drought event series, and therefore r_d and r_s were considered to be equal in this study ($r_d = r_s = r_{ds} = 0.3$) (Tallaksen et al., 2009).

(2) Matching of meteorological and hydrological drought events

The time taken to propagate a meteorological drought event into a hydrological drought event must be determined before multiple events can be matched. Therefore, the correlation coefficients were calculated between SPI values over multiple timescales (1–12 months) and for 1-month SRI values. The timescale with the highest correlation coefficient was then considered to represent the drought propagation time.

Propagation time t_p shows that a hydrological drought event is a response to meteorological conditions that prevailed over the past t_p months. Therefore, for each individual hydrological drought event (d_i, s_i, t_{si}, t_{ei}), the trigger interval corresponding to meteorological conditions ranged between t_p months before the start of the drought event ($t_{si} - t_p$) and the end of the drought event (t_{ei}). If the trigger intervals of two adjacent hydrological drought events overlapped, the trigger interval of the second drought event was adjusted to occur from the end of the first drought event ($t_{ei} - 1$) to the end of the second drought event. These relationships are expressed as follows:

$$\text{trigger interval} = \begin{cases} [t_{si} - t_p, t_{ei}], \textit{if } t_{si} - t_{ei-1} \ t_p \\ [t_{ei-1}, t_{ei}], \textit{if } t_{si} - t_{ei-1} < t_p \end{cases} \quad (2)$$

In terms of meteorological conditions, drought events (d_1, s_1), (d_2, s_2), …, (d_i, s_i) were treated as removing water from the studied basin, whereas wet events v_1, v_2, …, v_j were regarded as supplying water to the basin. Hence, based on a given interval, a matched meteorological drought could be represented as:

$$\begin{cases} d = \sum_{n=1}^{i} d_n \\ s = \sum_{n=1}^{i} s_n - \sum_{m=1}^{j} v_m \end{cases}, \quad (3)$$

where d and s are duration and severity of the matched meteorological drought event, respectively, and v_m is regarded as supplying water to the basin.

In general, some meteorological drought events cannot trigger hydrological drought due to the regulatory capacity of the watershed itself. Consequently, Sattar et al. (2019) proposed usage of the T_r to investigate the sensitivity of propagation from meteorological drought to hydrological drought, which is the ratio of the number of hydrological events to the number of meteorological drought events that occurred during a given period.

The modified equation for T_r used in this work was as follows:

$$T_r = \frac{m_p}{m_t} \times 100 \quad (4)$$

where m_p represents the number of meteorological drought events that triggered hydrological drought events and m_t is the total of meteorological drought events.

(3) The drought propagation threshold based on the Copula function

The Copula function can examine multiple drought characteristics simultaneously, and has been widely used to perform multivariate drought probabilistic analysis and to reveal drought propagation characteristics (*e.g.*, Vicente-Serrano et al., 2010; Sadegh et al., 2017; Guo et al., 2019b).

The Copula function can be expressed as:

$$C(u, v) = \varphi^{-1}(\varphi(u), \varphi(v)) \quad (5)$$

where C(u, v) is the Copula function combined with two random variables, φ denotes the convex function, and u and v represent the two variables.

The Copula method was combined with T_r to estimate the threshold for propagation from meteorological to hydrological drought *via* a three-stage analysis. (*i*) Firstly, the marginal distribution of random variables was determined. In this study, matched drought duration was used alongside the severity of meteorological and hydrological droughts to fit the marginal distribution. Four common functions were applied to fit the matched duration and severity data, including the Weibull (WEL) distribution, an exponential (EXP) distribution, a generalized extreme value (GEV) distribution, and a generalized Pareto (GP) distribution. Due to the application of a marginal distribution, the joint distribution was structured according to Eq. (5). (*ii*) Secondly, as the duration and severity of meteorological drought were selected as marginal variables to construct the joint distribution in this study, the Gaussian Copula, *t* Copula, Clayton Copula, Frank Copula, and Gumbel Copula methods were used to compare results against the empirical Copula distribution. The results of this analysis that showed the best fit were then quantitatively used to determine the square Euclidean distance (SED). (*iii*) Finally, the T_r was set as a target value and meteorological drought characteristics were treated as conditional variables. Robust meteorological drought characteristics can be deduced for any given value of T_r, with these characteristics serving as thresholds to trigger hydrological drought events in different watersheds. Furthermore, cumulative probability interval divisions were set as [0, 0.5], [0.5, 0.75], [0.75, 0.9], and [0.9, 1] for slight, moderate, severe, and extreme drought events, respectively (Guo et al., 2019a; Guo et al., 2019b). Then, the meteorological drought characteristics were assessed from these data, which were represented in terms of drought severity and duration.

2.3. Data description

Monthly Q during 1961–2016 were collected from the Ministry of Water Resources of China at eight gauges throughout the YRB, China, whereas monthly P values were collected from the National Meteorological Information Center (National Meteorological Information Center, 2018). In order to ensure that only reliable data were used, quality control was conducted on P and Q values prior to analysis. A dataset of gridded monthly P (0.5° × 0.5°) values during 1961–2016 in China was deduced from observations of P made at 2474 national ground stations. This gridding procedure employed the thin-disk spline method, and digital elevation data were introduced in order to eliminate the impact of elevation on the accuracy of spatial interpolation of P due to the unique terrain within China. Monthly P and Q values were used to estimate SPI and SSI, and then were used to explore drought propagation processes.

3. Results

3.1. Drought events detected by SPI and SSI

Response time, reflected by Correlation coefficients (PCC), showed two main patterns (Fig. 3). Firstly, the response times in different watersheds varied according to the timescales used for analysis; for example, response time ranged from 6 to 10 months for a 1-month SSI, and presented significant differences over different timescales ($p < 0.05$). Secondly, as expected, long hydrological droughts caused longer response times; for example, mean response times of 8.25, 10, 10.63, and 14.13 months were recorded for 1-month, 3-month, 6-month, and 12-month SSI values, respectively. The response time at the 1-month scale was used to match meteorological and hydrological drought events.

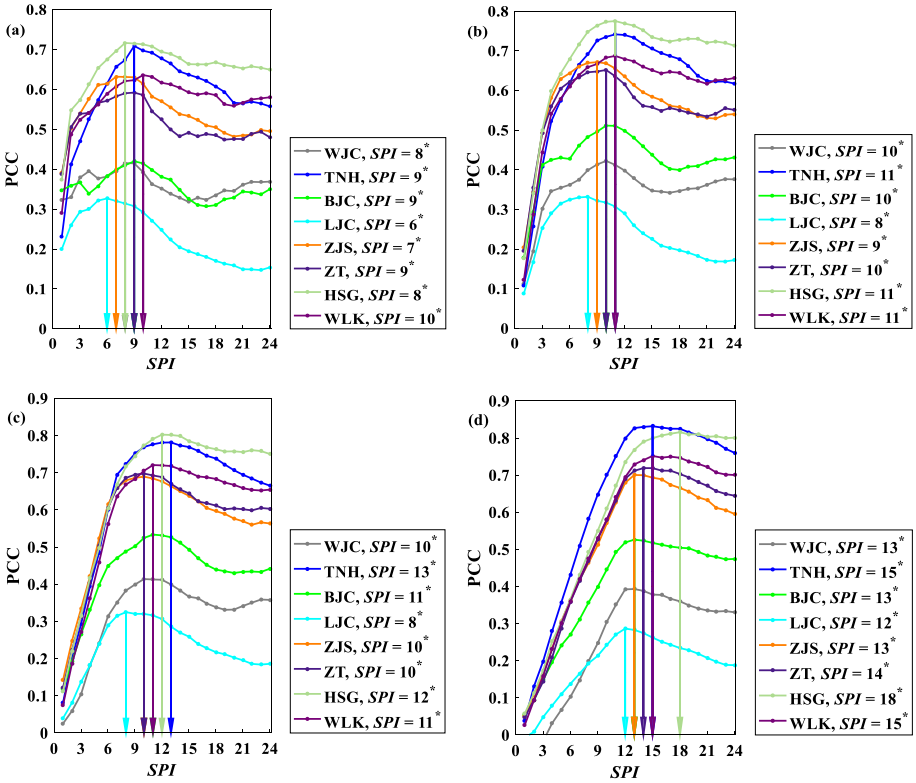

Fig. 3. Correlation coefficients (PCC) between single timescales of 1 month (a), 3 months (b), 6 months (c), and 12 months (d) with different timescales for the SPI (*e.g.*, from 1 to 24 months). The maximum correlation coefficients between SSI and SPI shown in the figures were used to estimate the response time.

Both of duration and severity transmitted from meteorological to hydrological drought presented consistent patterns (Fig. 4). As expected, duration and severity of meteorological drought amplified from their original measurements when transmitted to combined events and matched meteorological drought events, with all changes being statistically significant ($p < 0.01$, as shown by the Student's *t*-test) (Fig. 4a, b). For example, the mean meteorological durations for original, combined, and matched droughts in the WJC were 1.47, 1.60, and 1.64 months, respectively. Meanwhile, mean drought severity in the WJC enlarged from −1.63 for original drought events to −1.71 and −1.76 for combined and matched droughts, respectively. Hydrological drought events showed similar increases when converting from original events to combined drought events (Fig. 4c, d). Interestingly, both duration and severity were typically amplified for hydrological droughts than meteorological droughts. For example, original meteorological drought durations and severities in the WJC watershed were up to 1.47 months and −1.63, respectively, while original hydrological drought durations and severities were up to 2.79 months and –3.18, respectively. Finally, matched meteorological and hydrological droughts also showed similar amplified effects in different watersheds. For example, duration and severity of matched meteorological droughts in WJC were up to 1.64 months and −1.76, respectively, whereas these characteristics for matched hydrological droughts were up to 6.41 months and −7.09, respectively.

3.2. Transition from meteorological to hydrological drought

Number of original, pooled, and matched drought events identified during the study period demonstrated clear propagations from meteorological to hydrological drought (Table 1). The numbers of original to pooled, and pooled to matched meteorological drought events reduced with each transition, and similar reductions were identified for hydrological droughts. Values for T_r were inconsistent between watersheds, ranging from 43 % in the LJC watershed to 66 % in the TNH and BJC watersheds, and showing an average of 55 %.

Increases in hydrological drought durations and severities were further confirmed during propagation from meteorological to hydrological drought (Fig. 5). Both variables showed statistically significant increases ($p < 0.01$), with slopes of 1.67 and 1.45, respectively. These increases in duration and severity varied between watersheds; for example, duration ranged from 1.07 in the LJC to 2.16 in the WLK, whereas severity ranged from 1.02 in the LJC to 2.05 in the WLC. No significant increases were identified between duration and severity ($p = 0.04$, determined by the Student's *t*-test).

(3) Drought propagation threshold based on the Copula function

The RMSE resulted from four distributions (WEL, EXP, GEV, and GP) in fitting duration and severity data for original meteorological and hydrological drought events in eight watersheds showed that (Supplement Fig. 1): the best-fit distributions for both meteorological and hydrological drought severity were represented by the GEV, and RMSE were 0.04 and 0.05, respectively. While best-fit distributions for meteorological and hydrological drought durations were represented by the WBL (RMSE = 0.17, $p = 0.23$) and GEV (RMSE = 0.05, $p = 0.09$), respectively.

Duration and severity of meteorological drought events were selected as marginal variables to construct a joint distribution, and the Copula function was quantitatively used to obtain the SED value (Fig. 6). Results showed that the Gaussian Copula best described the joint distribution (SED = 0.04), which showed that slight, moderate, severe, and extreme meteorological droughts were differentiated in terms of their duration and severity (Table 2). As expected, drought severity and duration increased commensurately with an increase in drought extremity, while drought characteristics varied for droughts of the same extremity, but in different watersheds. Interestingly, the triggering threshold for drought severity and duration varied between watersheds, and duration thresholds were consistently larger for slight droughts. The drought severity threshold ranged from slight in the TNH and BJC watersheds to moderate in the other six watersheds.

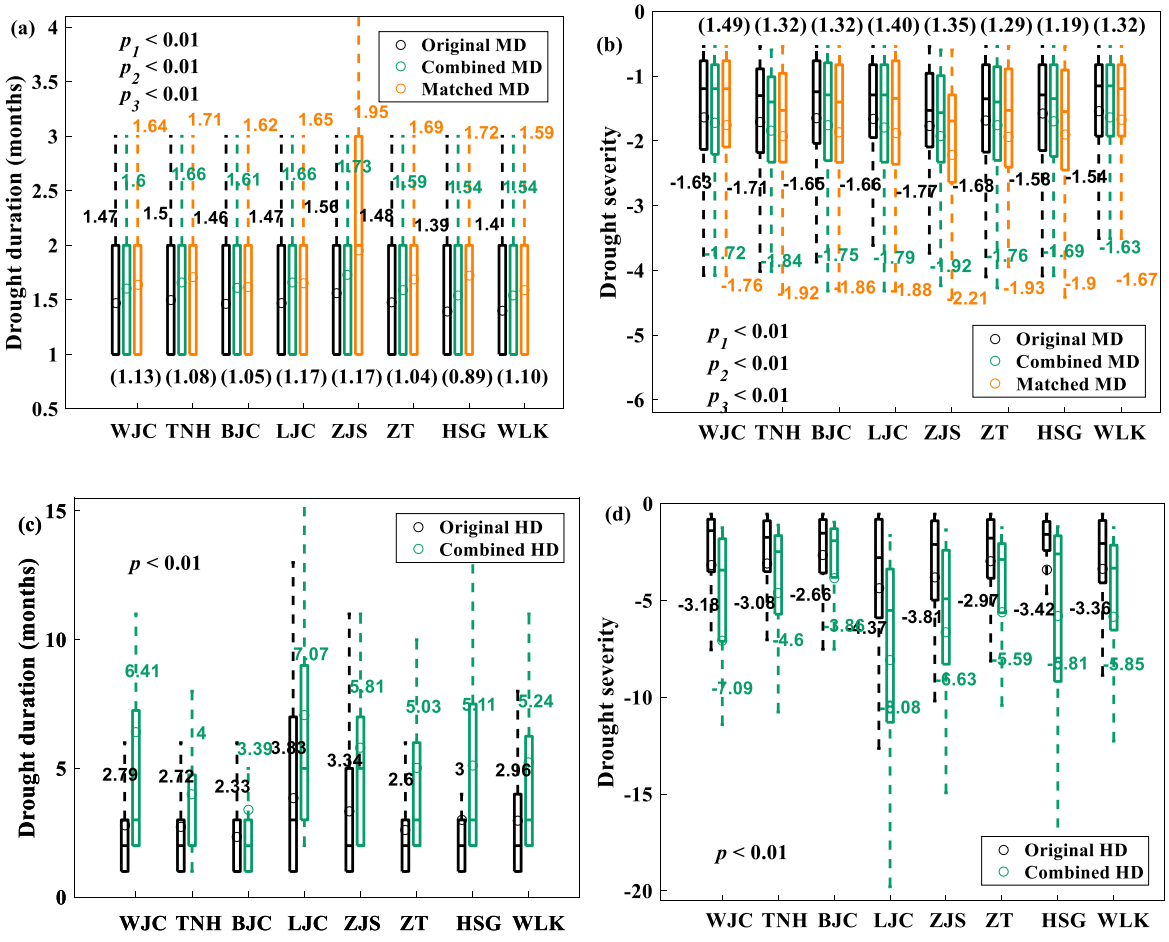

Fig. 4. Meteorological and hydrological drought characteristics for original events and those that were matched after pooling. Duration (a) and severity (b) for original meteorological and hydrological droughts, and duration (c) and severity (d) for matched meteorological and hydrological droughts, respectively, after pooling theory had been performed. The standard deviations (STD) were also showed in the Figure with bracket.

4. Discussion

4.1. The propagation of meteorological drought to hydrological drought

For the same observational timescale, response times for drought propagation obtained from SPI data showed notable variations between watersheds (Fig. 3). Such differences mainly arise from varying watershed characteristics, including its water storage capacity (*e.g.*, Yang et al., 2017; Peterson et al., 2021), and vegetation structure and function (*e.g.*, Vicente-Serrano et al., 2012; Liu et al., 2022). As shown in Supplementary Table 1, response time reduced when slope (-0.26) and κ (-0.36) increased, suggesting that the propagation from meteorological to hydrological drought occurs when slope values increase and watersheds decrease their water storage capacities. Changes to watershed water storage capacity and vegetation characteristics affect *P*–*Q* relationships (Saft et al., 2016; Peterson et al., 2021), and inevitably alter a watershed's response time. For example, deeper soil needs more time to respond than shallow soil, as shown by Z_e values in Supplementary Table 1. This is particularly true in watersheds with a large soil water storage capacity (Saft et al., 2016), which should also experience a pronounced change in their *P*–*Q* relationship. Some researchers have suggested that vegetation responds to drought events by increasing the fraction of *P* that is transpired (Peterson et al., 2021). This can be facilitated by a range of complex mechanisms induced by drought, such as widening the vadose zone and increasing soil capacity (Dunne and Black, 1970), changing soil hydraulic properties (Caplan et al., 2019), and/or vegetation phenology (*e.g.*, Ma et al., 2015). The partial area contribution mechanism (Dunne and Black, 1970; Saft et al., 2016) suggests that groundwater level regulates the fraction of *P* that can be converted to *Q*, and thus explains how watershed water storage plays a critical role in influencing response time. Generally, a longer response time implies that duration and severity of a meteorological drought regime will have a greater effect on the subsequent hydrological drought regime, in turn indicating a higher T_r. The opposite scenario was also observed, whereby a shorter response time in the LJC and ZJS watersheds was associated with a smaller T_r.

Table 1
Numbers of original, pooled, and matched meteorological drought (MD) and hydrological drought (HD) events, and transition rates (T_r, %) for different watersheds.

Drought		WJC	TNH	BJC	LJC	ZJS	ZT	HSG	WLK
Original	MD	138	136	140	139	130	138	147	146
	HD	73	74	87	53	60	77	67	69
Pooled	MD	131	125	132	129	120	132	138	138
	HD	29	47	56	27	32	38	36	37
Matched	MD	67	90	93	60	61	77	83	86
T_r (%)		49	66	66	43	47	56	56	59

Matched meteorological and hydrological droughts were determined using run theory, and were detected in order to verify the changes in severity and duration for original drought events (Fig. 4). This treatment indicated that hydrological drought must be triggered by a severe meteorological drought, and that 45 % of original meteorological drought lost its strength in inducing apparent hydrological drought (Table 1). Differences in the standard deviation (STD) according to drought regime (*i.e.*, in terms of severity and duration) can partly explain the differences in T_r between watersheds (Fig. 4). Higher STD values imply larger differences in both meteorological drought duration and severity, suggesting that minor

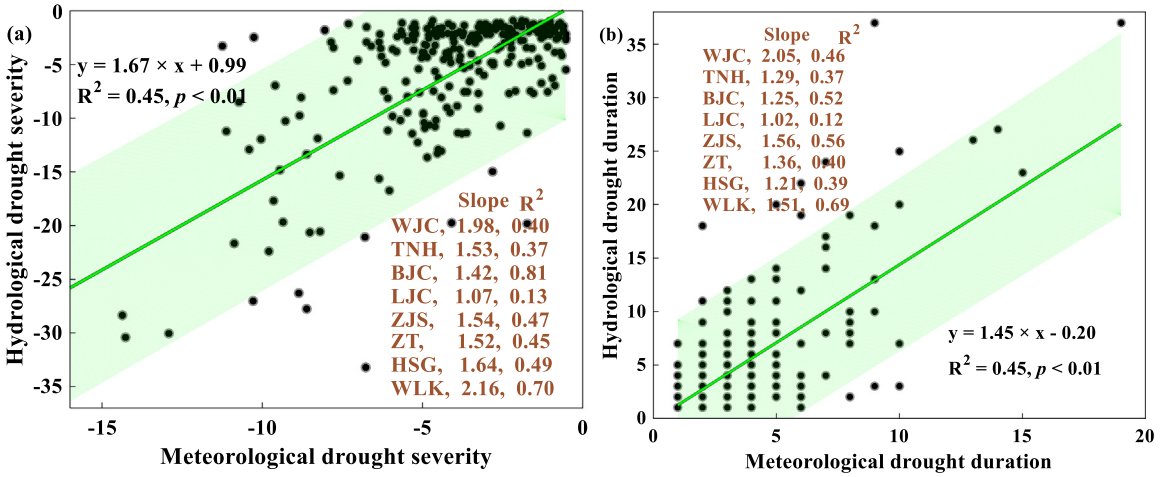

Fig. 5. Relationships between severity (a) and duration (b) for meteorological and hydrological drought events. Linear fitted models and derivative equations, R^2 values, and slopes for each watershed are also shown.

drought events eventually reduce T_r; for example, drought duration and severity values of 1.13 and 1.49 for the WJC, 1.17 and 1.40 for the LJC, 1.17 and 1.35 for the ZJS induced smaller T_r values of 49 %, 43 %, and 47 % for the same watersheds, respectively. Guo et al. (2020) argued that minor drought events and large supply events eventually lead to low T_r values; however, the amplification effects reported here that relate to hydrological events triggering meteorological drought events (Fig. 5) suggest a non-proportional reduction in Q with a multi-year reduction in P (Yang et al., 2017; Konapala and Mishra, 2020; Peterson et al., 2021). As was noted by Apurv and Cai (2020), a storage–discharge relationship is a key watershed property that controls the intensity of hydrological droughts. In general, a wetter climate is associated with a lower severity and intensity of hydrological drought, and such a watershed is more likely to recover from drought (Liu et al., 2023). Differences in the propagation threshold further validated the non-proportional reduction in Q with reduction in P (Table 2). For example, the WJC, LJC, and ZJS watersheds recorded a higher propagation threshold for both drought duration and severity. Nonetheless, attempts to define drought, which mainly relate to the diversity of drought indices – and even the same drought indices considered over different timescales – will inevitably introduce uncertainty into interpretation of thresholds, and will cause disagreements between different drought assessments (*e.g.*, Satoh et al., 2021; Wu et al., 2021a). Importantly, the triggering thresholds for meteorological drought indicate that *P*–*Q* relationships shift, which implies that hydrological drought will also induce a shift in *P*–*Q* relationships (Saft et al., 2016; Wu et al., 2021b). Mechanisms that control a watershed's recovery after a period of drought have been explained by threshold switching characteristics combined with traditional bucket water model (Liu et al., 2023). That is to say, vegetation prioritizes water use, which regulates *P* partitioning, and thus controls the shift in *P*–*Q* relationship.

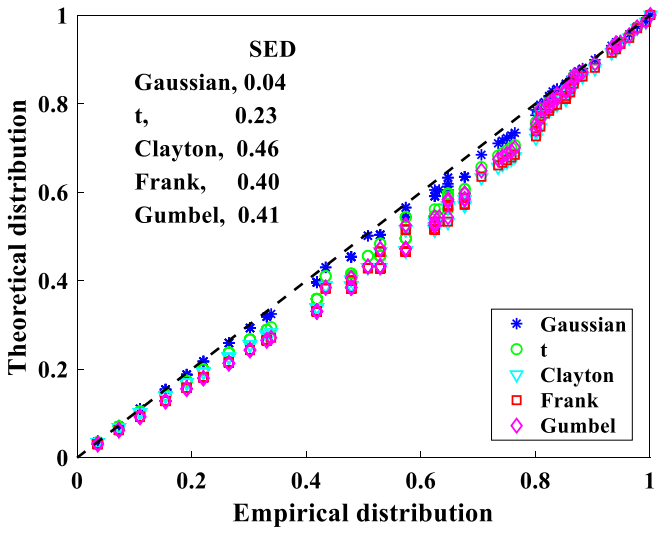

Fig. 6. P-P plots of empirical and theoretical CDFs of different Copula methods, alongside the results of their quantitative goodness-of-fit tests (WJC watershed as an example).

4.2. Uncertainties and further research

Induced by the drought event, *P*–*Q* relationship presents nonlinear response (Saft et al., 2016; Liu et al., 2023). As pointed by Peterson et al. (2021), watersheds may have multiple steady states in Q response even when P deficit has recovered (Peterson et al., 2021), implying threshold for propagation should vary with watershed states while assumed as steady state in present study. Declines in terrestrial water storage, mainly induced by climate changes, transmit to increases in future droughts (Pokhrel et al., 2021). Human activities, such as revegetation activities, hydrological engineering, and irrigation, might alter the Q. For example, "Grain-for-Green Project" has induced dramatic changes in vegetation on the Loess Plateau of Yellow River Basin, which induced a series of alteration in hydrological cycles, *e.g.*, more portion of P into soil water storage to maintain higher evapotranspiration (Zhou et al., 2022), and even approaching sustainable water resource limits (Feng et al., 2016).

Table 2
Propagation thresholds for drought severities and durations when transitioning from meteorological to hydrological drought. Drought severity and duration variables for slight, moderate, severe, and extreme drought events are also shown.

	WJC	TNH	BJC	LJC	ZJS	ZT	HSG	WLK
Drought severity								
Slight	1.40	1.44	1.42	1.41	1.50	1.43	1.36	1.34
Moderate	2.31	2.31	2.34	2.29	2.39	2.34	2.16	2.21
Severe	3.70	3.36	3.69	3.50	3.41	3.54	3.09	3.47
Extreme	6.67	5.20	6.35	5.76	5.07	5.76	4.62	6.03
Threshold	2.21	1.43	1.21	1.81	1.95	1.59	1.52	1.70
Drought duration (months)								
Slight	1.27	1.31	1.26	1.27	1.35	1.28	1.24	1.23
Moderate	2.03	2.07	2.01	2.03	2.16	2.05	1.84	1.89
Severe	2.58	2.60	2.55	2.56	2.73	2.60	2.21	2.33
Extreme	3.15	3.14	3.09	3.11	3.32	3.17	2.57	2.78
Threshold	1.96	1.47	1.35	1.86	1.92	1.64	1.52	1.61

Drought events, controlled by complex coupled climate system, present spatially compounding characteristics under changing dynamic and thermodynamic conditions, implicating the possibility of simultaneous larger-scale droughts over multiple continents (Mondal et al., 2023). Meanwhile, land-atmosphere coupling effects closely interact with drought evolution, which will inevitably induced a series of climate hazards (*e.g.*, heatwaves) and aggravated effect in uneven distribution of water resources (Yin et al., 2022b). As droughts are occurring more frequently and atmospheric warming triggers stronger land–atmosphere feedback, the compound drought–heatwave events have drawn attentions (Yin et al., 2023). The mechanisms of compound drought–heatwave events have been explained as: (*i*) extreme hot temperatures have become increasingly synchronized with drought conditions worldwide, as drier land during heatwaves increases the surface temperature; and (*ii*) heatwaves may be amplified through pulses of heat advection from anomalously dry regions upwind (Yin et al., 2022a). Although several uncertainties will limit the accuracy of threshold for triggering the propagation of meteorological drought to hydrological drought, it still can provide an indicator to help address impact of drought. Further research should be paid more attention to detect and analyzing effects of human activities on drought propagation and its relative climatic hazard (*e.g.*, heatwaves), which will help to mitigate the impact of drought on ecosystem, and socioeconomic system.

5. Conclusions

The propagation thresholds that trigger a transition from meteorological drought to hydrological drought are incompletely understood, which hinders effective establishment of drought warning systems and prevention measures. Here, propagation thresholds were assessed by identifying drought events in different watersheds from a typical water-limited region in China, subsequently pooling, excluding, and matching them, and then assessing their propagation thresholds by using a Copula function and T_r analysis. Three main conclusions can be drawn:

(i) Response time varied significantly with different timescales ($p < 0.5$) in different watersheds. Interestingly, the response time increased alongside the studied timescales, and combined meteorological and hydrological drought characteristics were severe when compared with data for original events.

(ii) Values for T_r ranged from 43 % (LJC) to 66 % (TNH and BJC) between different watersheds, and robust amplification occurred between matching meteorological and hydrological droughts, with linear fits having slopes of 1.67 and 1.45 for drought severity and duration, respectively.

(iii) Shorter response times correlated with smaller T_r values of 43 % and 47 % in the LJC and ZJS watersheds respectively, and also higher propagation thresholds in drought characteristics (*e.g.*, 1.81 and 1.95 for drought severity in the LJC and ZJS, respectively). These relationships suggest that a shorter response time tends to generate a more extreme hydrological drought regime with a lower T_r, and *vice versa*. These results provide critical new insight into how propagation thresholds affect drought events, and will ultimately aid management of water resources in the YRB and can help to mitigate the effects of future climate change.

Supplementary data to this article can be found online at https://doi.org/10.1016/j.scitotenv.2023.162771.

CRediT authorship contribution statement

Qiang Liu: Conceptualization, Supervision, Writing - Reviewing and Editing; **Liqiao Liang**: Methodology, Software, Data curation, Writing - Original draft preparation; **Yuting Yang:** Editing; **Jun He**, Methodology; **Denghua Yan**, Data curation, methodology; **Xuan Wang**, Visualization, Investigation; **Chunhui Li**, Visualization, Investigation; T**ao Sun**, Visualization, Investigation.

Data availability

The data that has been used is confidential.

Declaration of competing interest

The authors declare that they have no known competing financial interests or personal relationships that could have appeared to influence the work reported in this paper.

Acknowledgements

We gratefully acknowledge the Yellow River Conservancy Commission (YRCC) for offering the observed streamflow. This study was financially supported by the National Natural Science Foundation of China (No. 42071129, 42271141), and the National Key Basic Research and Development Project (No. 2022YFF1300902). All data used in this study have been properly cited and referenced below.

References

Allen, R.G., Pereira, L.S., Raes, D., 1998. Crop evapotranspiration—guidelines for computing crop water requirements. FAO Irrigation and Drainage Paper 56. FAO ISBN 92-5-104219-5, 326 pp.

American Meteorological Society, 1997. Meteorological drought-policy statement. Bull. Am. Meteorol. Soc. 78, 847–849.

Apurv, T., Cai, X., 2020. Drought propagation in contiguous U.S. Watersheds: a process-based understanding of the role of climate and watershed properties. Water Resour. Res. 56 (9). https://doi.org/10.1029/2020wr027755.

Apurv, T., Sivapalan, M., Cai, X., 2017. Understanding the role of climate characteristics in drought propagation. Water Resour. Res. 53 (11), 9304–9329. https://doi.org/10.1002/2017wr021445.

Azhdari, Z., Bazrafshan, O., Shekari, M., et al., 2020. Three-dimensional risk analysis of hydro-meteorological drought using multivariate nonlinear index. Theor. Appl. Climatol. 142 (3–4), 1311–1327. https://doi.org/10.1007/s00704-020-03365-3.

Azhdari, Z., Bazrafshan, O., Zamani, H., et al., 2021. Hydro-meteorological drought risk assessment using linear and nonlinear multivariate methods. Phys. Chem. Earth A/B/C 123. https://doi.org/10.1016/j.pce.2021.103046.

Beck, H.E., van Dijk, A.I.J.M., Levizzani, V., et al., 2016. MSWEP: 3-hourly 0.25 global gridded precipitation (1979–2015) by merging gauge, satellite, and reanalysis data. Hydrol. Earth Syst. Sci. Discuss. https://doi.org/10.5194/hess-21-589-2017.

Caplan, J.S., Gimenez, D., Hirmas, D.R., 2019. Decadal-scale shifts in soil hydraulic properties as induced by altered precipitation. Sci. Adv. 5 (9), eaau6635. https://doi.org/10.1126/sciadv.aau6635.

Chang, J.X., Li, Y.Y., Wang, Y.M., et al., 2016. Copula-based drought risk assessment combined with an integrated index in the Wei River Basin, China. J. Hydrol. 540, 824–834. https://doi.org/10.1016/j.jhydrol.2016.06.064.

Dai, A., 2012. Increasing drought under global warming in observations and models. Nat. Clim. Chang. 3 (1), 52–58. https://doi.org/10.1038/nclimate1633.

Dai, M., Huang, S.Z., Huang, Q., et al., 2020. Assessing agricultural drought risk and its dynamic evolution characteristics. Agric. Water Manag. 231. https://doi.org/10.1016/j.agwat.2020.106003.

Dunne, T., Black, R.D., 1970. Partial area contributions to storm runoff in a small New-England watershed. Water Resour. Res. 6 (5), 1296–1311. https://doi.org/10.1029/WR006i005p01296.

FAO/IIASA/ISIRC/ISS-CAS/JRC, 2008. Harmonized World Soil Database (Version 1.0). FAO, Rome, Italy and IIASA, Laxenburg, Austria.

Farahmand, A., AghaKouchak, A., 2015. A generalized framework for deriving nonparametric standardized drought indicators. Adv. Water Resour. 76, 140–145. https://doi.org/10.1016/j.advwatres.2014.11.012.

Feng, X., Fu, B., Piao, S., et al., 2016. Revegetation in China's loess plateau is approaching sustainable water resource limits. Nat. Clim. Chang. 6 (11), 1019–1022. https://doi.org/10.1038/nclimate3092.

Guo, Y., Huang, S.Z., Huang, Q., et al., 2019a. Assessing socioeconomic drought based on an improved multivariate standardized reliability and resilience index. J. Hydrol. 568, 904–918. https://doi.org/10.1016/j.jhydrol.2018.11.055.

Guo, Y., Huang, S., Huang, Q., et al., 2019b. Copulas-based bivariate socioeconomic drought dynamic risk assessment in a changing environment. J. Hydrol. 575, 1052–1064. https://doi.org/10.1016/j.jhydrol.2019.06.010.

Guo, Y., Huang, S.Z., Huang, Q., et al., 2020. Propagation thresholds of meteorological drought for triggering hydrological drought at various levels. Sci. Total Environ. 712. https://doi.org/10.1016/j.scitotenv.2020.136502.

Han, D., Deng, J., Gu, C., et al., 2021. Effect of shrub-grass vegetation coverage and slope gradient on runoff and sediment yield under simulated rainfall. Int. J. Sediment Res. 36 (1), 29–37. https://doi.org/10.1016/j.ijsrc.2020.05.004.

Hao, Z., AghaKouchak, A., Nakhjiri, N., et al., 2014. Global integrated drought monitoring and prediction system. Sci. Data 1, 140001. https://doi.org/10.1038/sdata.2014.1.
Huang, S., Huang, Q., Chang, J., et al., 2016. Linkages between hydrological drought, climate indices and human activities: a case study in the Columbia River basin. Int. J. Climatol. 36 (1), 280–290. https://doi.org/10.1002/joc.4344.
Konapala, G., Mishra, A., 2020. Quantifying climate and catchment control on hydrological drought in the continental United States. Water Resour. Res. 56 (1). https://doi.org/10.1029/2018WR024620.
Liang, K., Bai, P., Li, J.J., et al., 2014. Variability of temperature extremes in the Yellow River basin during 1961–2011. Quat. Int. 336, 52–64. https://doi.org/10.1016/j.quaint.2014.02.007.
Liang, W., Bai, D., Wang, F.Y., et al., 2015. Quantifying the impacts of climate change and ecological restoration on streamflow changes based on a budyko hydrological model in China's loess plateau. Water Resour. Res. 51 (8), 6500–6519. https://doi.org/10.1002/2014WR016589.
Liu, Q., Yang, Z., Cui, B., 2008. Spatial and temporal variability of annual precipitation during 1961–2006 in Yellow River Basin, China. J. Hydrol. 361 (3-4), 330–338. https://doi.org/10.1016/j.jhydrol.2008.08.002.
Liu, Q., McVicar, T.R., Yang, Z.F., et al., 2016. The hydrological effects of varying vegetation characteristics in a temperate water-limited basin: development of the dynamic budyko-choudhury-porporato (dBCP) model. J. Hydrol. 543, 595–611. https://doi.org/10.1016/j.jhydrol.2016.10.035.
Liu, Q., Yang, Y., Liang, L., et al., 2022. Hydrological effects of the snow fraction and its ecohydrological explication within the budyko framework. J. Hydrol. 610. https://doi.org/10.1016/j.jhydrol.2022.127813.
Liu, Q., Yang, Y., Liang, L., et al., 2023. Shift in precipitation-streamflow relationship induced by multi-year drought across global catchments. Sci. Total Environ. 857 (Pt 2), 159560. https://doi.org/10.1016/j.scitotenv.2022.159560.
Ma, X., Huete, A., Moran, S., et al., 2015. Abrupt shifts in phenology and vegetation productivity under climate extremes. J. Geophys. Res. Biogeosci. 120 (10), 2036–2052. https://doi.org/10.1002/2015jg003144.
Madadgar, S., AghaKouchak, A., Farahmand, A., et al., 2017. Probabilistic estimates of drought impacts on agricultural production. Geophys. Res. Lett. 44 (15), 7799–7807. https://doi.org/10.1002/2017gl073606.
Madsen, H., Rosbjerg, D., 1995. On the Modelling of Extreme Droughts. IAHS-AISH Publ, pp. 377–385.
Mao, J., Yan, B., 2019. Global Monthly Mean Leaf Area Index Climatology, 1981-2015. ORNL DAAC, Oak Ridge, Tennessee, USA https://doi.org/10.3334/ORNLDAAC/1653.
McKee, T.B., Doesken, N.J., Kleist, J., 1993. The relationship of drought frequency and duration to time scale. Eighth Conference on Applied Climatology, Anaheim California. 17, pp. 179–184.
McVicar, T.R., Li, L., Van Niel, T.G., et al., 2007. Developing a decision support tool for China's re-vegetation program: simulating regional impacts of afforestation on average annual streamflow in the loess plateau. For. Ecol. Manag. 251 (1–2), 65–81. https://doi.org/10.1016/j.foreco.2007.06.025.
McVicar, T.R., Van Niel, T.G., Roderick, M.L., et al., 2010. Observational evidence from two mountainous regions that near-surface wind speeds are declining more rapidly at higher elevations than lower elevations: 1960–2006. Geophys. Res. Lett. 37 (6), L06402. https://doi.org/10.1029/2009gl042255.
Mondal, S., Mondal, A.K., Leung, R., et al., 2023. Global droughts connected by linkages between drought hubs. Nat. Commun. 14 (1), 144. https://doi.org/10.1038/s41467-022-35531-8.
Montaseri, M., Amirataee, B., Rezaie, H., 2018. New approach in bivariate drought duration and severity analysis. J. Hydrol. 559, 166–181. https://doi.org/10.1016/j.jhydrol.2018.02.018.
National Meteorological Information Center, 2018. Dataset of gridded monthly precipitation in China (Version 2.0) (1961-2018). http://data.cma.cn/.
Palmer, W.C., 1965. Meteorological Drought. Research Paper 45, U.S. Dept. of Commerce, pp. 1–58.
Penman, H.L., 1948. Natural evaporation from open water, bare soil and grass. Proc. R. Soc. Lond. 193 (1032), 120–145.
Peterson, T.J., Saft, M., Peel, M.C., et al., 2021. Watersheds may not recover from drought. Science 372 (6543), 745–749. https://doi.org/10.1126/science.abd5085.
Piao, S., Yin, G., Tan, J., et al., 2015. Detection and attribution of vegetation greening trend in China over the last 30 years. Glob. Chang. Biol. 21 (4), 1601–1609. https://doi.org/10.1111/gcb.12795.
Pokhrel, Y., Felfelani, F., Satoh, Y., et al., 2021. Global terrestrial water storage and drought severity under climate change. Nat. Clim. Chang. 11 (3), 226–233. https://doi.org/10.1038/s41558-020-00972-w.
Sadegh, M., Ragno, E., AghaKouchak, A., 2017. Multivariate copula analysis toolbox (MvCAT): describing dependence and underlying uncertainty using a bayesian framework. Water Resour. Res. 53 (6), 5166–5183. https://doi.org/10.1002/2016wr020242.
Sadeghipour, J., Dracup, J.A., 1985. Regional frequency-analysis of hydrologic multiyear droughts. Water Resour. Bull. 21 (3), 481–487. https://doi.org/10.1016/0022-1694(85)90197-0.
Saft, M., Peel, M.C., Western, A.W., et al., 2016. Predicting shifts in rainfall-runoff partitioning during multiyear drought: roles of dry period and catchment characteristics. Water Resour. Res. 52 (12), 9290–9305. https://doi.org/10.1002/2016wr019525.
Samaniego, L., Kumar, R., Zink, M., 2013. Implications of parameter uncertainty on soil moisture drought analysis in Germany. J. Hydrometeorol. 14 (1), 47–68. https://doi.org/10.1175/Jhm-D-12-075.1.
Satoh, Y., Shiogama, H., Hanasaki, N., et al., 2021. A quantitative evaluation of the issue of drought definition: a source of disagreement in future drought assessments. Environ. Res. Lett. 16 (10). https://doi.org/10.1088/1748-9326/ac2348.
Satoh, Y., Yoshimura, K., Pokhrel, Y., et al., 2022. The timing of unprecedented hydrological drought under climate change. Nat. Commun. 13 (1), 3287. https://doi.org/10.1038/s41467-022-30729-2.
Sattar, M.N., Lee, J.Y., Shin, J.Y., et al., 2019. Probabilistic characteristics of drought propagation from meteorological to hydrological drought in South Korea. Water Resour. Manag. 33 (7), 2439–2452. https://doi.org/10.1007/s11269-019-02278-9.
Shukla, S., Wood, A.W., 2008. Use of a standardized runoff index for characterizing hydrologic drought. Geophys. Res. Lett. 35 (2). https://doi.org/10.1029/2007gl032487.
Shuttleworth, W.J., 1993. Evaporation. In: Maidment, D.R. (Ed.), Handbook of Hydrology. McGraw-Hill, Sydney (Chapter 4).
Tallaksen, L.M., Madsen, H., Clausen, B., 2009. On the definition and modelling of streamflow drought duration and deficit volume. Hydrol. Sci. J. 42 (1), 15–33. https://doi.org/10.1080/02626669709492003.
Trenberth, K.E., Dai, A., van der Schrier, G., et al., 2013. Global warming and changes in drought. Nat. Clim. Chang. 4 (1), 17–22. https://doi.org/10.1038/nclimate2067.
Tu, X., Wu, H., Singh, V.P., et al., 2018. Multivariate design of socioeconomic drought and impact of water reservoirs. J. Hydrol. 566, 192–204. https://doi.org/10.1016/j.jhydrol.2018.09.012.
Tu, X., Du, Y., Singh, V.P., et al., 2019. Bivariate design of hydrological droughts and their alterations under a changing environment. J. Hydrol. Eng. 24 (6). https://doi.org/10.1061/(asce)he.1943-5584.0001788.
Van Loon, A.F., Gleeson, T., Clark, J., et al., 2016. Drought in the anthropocene. Nat. Geosci. 9 (2), 89–91. https://doi.org/10.1038/ngeo2646.
Vicente-Serrano, S.M., Begueria, S., Lopez-Moreno, J.I., 2010. A multiscalar drought index sensitive to global warming: the standardized precipitation evapotranspiration index. J. Clim. 23 (7), 1696–1718. https://doi.org/10.1175/2009jcli2909.1.
Vicente-Serrano, S.M., Gouveia, C., Camarero, J.J., et al., 2012. Response of vegetation to drought time-scales across global land biomes. Proc. Natl. Acad. Sci. 110 (1), 52–57. https://doi.org/10.1073/pnas.1207068110.
Wang, D., Wang, L., 2018. Canopy interception of apple orchards should not be ignored when assessing evapotranspiration partitioning on the loess plateau in China. Hydrol. Process. 33 (3), 372–382. https://doi.org/10.1002/hyp.13330.
Wu, J., Chen, X., Yao, H., et al., 2017. Non-linear relationship of hydrological drought responding to meteorological drought and impact of a large reservoir. J. Hydrol. 551, 495–507. https://doi.org/10.1016/j.jhydrol.2017.06.029.
Wu, J., Miao, C., Zheng, H., et al., 2018. Meteorological and hydrological drought on the loess plateau, China: evolutionary characteristics, impact, and propagation. J. Geophys. Res. Atmos. 123 (20), 11569–11584. https://doi.org/10.1029/2018jd029145.
Wu, J.F., Chen, X.H., Yuan, X., et al., 2021a. The interactions between hydrological drought evolution and precipitation-streamflow relationship. J. Hydrol. 597 (126210). https://doi.org/10.1016/j.jhydrol.2021.126210.
Wu, J., Chen, X., Yao, H., et al., 2021b. Multi-timescale assessment of propagation thresholds from meteorological to hydrological drought. Sci. Total Environ. 765 (144232). https://doi.org/10.1016/j.scitotenv.2020.144232.
Wu, J., Yao, H., Chen, X., et al., 2022a. A framework for assessing compound drought events from a drought propagation perspective. J. Hydrol. 604. https://doi.org/10.1016/j.jhydrol.2021.127228.
Wu, G., Chen, J., Shi, X., 2022b. Impacts of global climate warming on meteorological and hydrological droughts and their propagations. Earth's Future 10 (3). https://doi.org/10.1029/2021ef002542.
Yan, S., Li, M., Sun, T., et al., 2021. The complex drought effects associated with the regulation of water-use efficiency in a temperate water-limited basin. J. Hydrol. Reg. Stud. 36. https://doi.org/10.1016/j.ejrh.2021.100864.
Yang, Y., Donohue, R.J., McVicar, T.R., 2016. Global estimation of effective plant rooting depth: implications for hydrological modeling. Water Resour. Res. 52 (10), 8260–8276. https://doi.org/10.1002/2016wr019392.
Yang, Y., McVicar, T.R., Donohue, R.J., et al., 2017. Lags in hydrologic recovery following an extreme drought: assessing the roles of climate and catchment characteristics. Water Resour. Res. 53 (6), 4821–4837. https://doi.org/10.1002/2017wr020683.
Yang, Y.T., Zhang, S.L., Roderick, M.L., et al., 2020. Comparing palmer drought severity index drought assessments using the traditional offline approach with direct climate model outputs. Hydrol. Earth Syst. Sci. 24 (6), 2921–2930. https://doi.org/10.5194/hess-24-2921-2020.
Yevjevich, V.M., 1967. An objective approach to definitions and investigations of continental hydrologic droughts. Hydrologic Paper. Colorado State Univ, Fort Collins, CO.
Yin, J., Slater, L., Gu, L., et al., 2022a. Global increases in lethal compound heat stress: hydrological drought hazards under climate change. Geophys. Res. Lett. 49 (18). https://doi.org/10.1029/2022gl100880.
Yin, J., Guo, S., Yang, Y., et al., 2022b. Projection of droughts and their socioeconomic exposures based on terrestrial water storage anomaly over China. Sci. China Earth Sci. 65 (9), 1772–1787. https://doi.org/10.1007/s11430-021-9927-x.
Yin, J., Gentine, P., Slater, L., et al., 2023. Future socio-ecosystem productivity threatened by compound drought–heatwave events. Nat. Sustain. https://doi.org/10.1038/s41893-022-01024-1.
Zelenhasić, E., Salvai, A., 1987. A method of streamflow drought analysis. Water Resour. Res. 23 (1), 156–168. https://doi.org/10.1029/WR023i001p00156.
Zhou, Z., Shi, H., Fu, Q., et al., 2021. Investigating the propagation from meteorological to hydrological drought by introducing the nonlinear dependence with directed information transfer index. Water Resour. Res. 57 (8). https://doi.org/10.1029/2021wr030028.
Zhou, J., Liu, Q., Liang, L., et al., 2022. More portion of precipitation into soil water storage to maintain higher evapotranspiration induced by revegetation on China's loess plateau. J. Hydrol. 615. https://doi.org/10.1016/j.jhydrol.2022.128707.